JOURNAL OF MATERIALS SCIENCE **36** (2001) 2329–2334

Spark-plasma-sintering of fine $BaTiO_3$ powder prepared by a sol-crystal method

TOMONARI TAKEUCHI[*]
National Institute of Advanced Industrial Science and Technology, AIST, Midorigaoka 1-8-31, Ikeda, Osaka, 563-8577, Japan
E-mail: takeuchi@onri.go.jp

YOKO SUYAMA
Shimane University, Matsue, Shimane, 690-8504, Japan

DEREK C. SINCLAIR
Department of Engineering Materials, University of Sheffield, Mappin Street, Sheffield, S1 3JD, UK

HIROYUKI KAGEYAMA
National Institute of Advanced Industrial Science and Technology, AIST, Midorigaoka 1-8-31, Ikeda, Osaka, 563-8577, Japan

Spark-Plasma-Sintering (SPS) has been applied to fine $BaTiO_3$ powder (several nanometers) prepared by a sol-crystal method. The starting powder was densified to more than 95% of the theoretical X-ray density, and the obtained SPS pellets had an average grain size of less than 1 μm, owning to the relatively low sintering temperature (900–1000°C) and short sintering period of ca. 3 min. The room temperature permittivity at 1 kHz for SPS samples sintered at 1000°C is ca. 10,000. This high room temperature permittivity value is attributed to electrical inhomogeneities within pellets; a resistive surface layer covers the inner pellet core that consists of oxygen-deficient $BaTiO_3$. The reduced pellet core is characteristic of SPS pellets formed from powders that contain small amounts of residual organic matter. © *2001 Kluwer Academic Publishers*

1. Introduction

Barium titanate ($BaTiO_3$) is a well known ferroelectric material with a high room temperature permittivity value, ca. >1000, and will continue to be used in the manufacture of thermistors, multilayer capacitors, electro-optic devices and DRAM (dynamic random access memories) into the twenty first century [1]. Improved performance, high permittivities and miniaturization of $BaTiO_3$-based devices can be achieved by controlling the ceramic microstructure such as grain size and homogeneity, which depends on the properties of the starting $BaTiO_3$ powder and sintering method [2]. In particular, grain size is one of the most important factors affecting the permittivity of $BaTiO_3$ ceramics; it has been widely reported that the room temperature permittivity at 1 kHz for $BaTiO_3$ ceramics shows an apparent maximum at grain size of ca. 1 μm [3–12]. Therefore, controlling the grain size to ca. 1 μm is advantageous in the production of high permittivity $BaTiO_3$-based devices.

It is well known that $BaTiO_3$ undergoes exaggerated grain growth during conventional sintering in a muffle furnace at elevated temperatures and long sintering periods [2]. Oonishi *et al.* [13] prepared dense $BaTiO_3$ ceramics (>98% of the theoretical X-ray density) with submicron grains (0.2–0.6 μm) by hot isostatic pressing (HIP). They applied 500 MPa to the powders during sintering, which was sufficient to decrease the c/a-ratio of the tetragonal unit cell, the Curie temperature and permittivity of $BaTiO_3$ ceramics [14, 15].

Spark-Plasma-Sintering (SPS) is a process which makes use of microscopic electrical discharge between particles under pressure (ca. 30 MPa) [16–18]. Although SPS is commonly used to produce dense metal and engineering ceramics, there are relatively few reports on the application of this technique to produce dense oxide-based electroceramics. The SPS process enables a compact powder to be sintered under uniform heating to high density at relatively lower temperatures and in much shorter sintering periods, typically a few minutes, compared with conventional sintering of cold-isostatic pressed (CIP) pellets [16–18]. The short sintering periods carried out in the SPS process are advantageous in suppressing exaggerated grain growth. Recently, we applied this technique to fine (0.1–0.6 μm) $BaTiO_3$ powders prepared by hydrothermal/hydrolysis methods and obtained dense (>95% of the theoretical X-ray density) ceramics with submicron grains [19, 20].

---

[*] Author to whom all correspondence should be addressed.

In addition to the sintering method, electrical properties of $BaTiO_3$-based devices depend on the homogeneity, composition and particle size of the starting powder [2]. Recently, we have obtained fine $BaTiO_3$ powder (several nanometers) by decomposition of organometallic crystals (sol-crystal method) [21]. In a mixed barium titanium double isopropoxide solution, transparent, square and plate-like single crystals ranging in size from a few millimeters to 1 cm, whose composition was presumed to be $BaTi[OCH(CH_3)_2]_6 \cdot C_6H_6$, grew at ca. 5°C, and they were converted to fine $BaTiO_3$ powder in air at relatively lower temperature, ca. 100°C, compared with that of similar single crystals of barium titanium double alkoxide solution [21–23]. The present $BaTiO_3$ prepared by a sol-crystal method shows relatively high permittivity (3700 at room temperature at 1 kHz), due probably to homogeneous cation stoichiometry and fine grains [24]. Combining the sol-crystal method to prepare stoichiometric fine powder and spark-plasma-sintering to produce dense ceramics of small and uniform grain size may lead to the production of $BaTiO_3$-based devices with much high/optimized permittivity characteristics.

In the present work, spark-plasma-sintering of $BaTiO_3$ powders (several nanometers) prepared by a sol-crystal method is reported. The density, grain size and electrical properties of the SPS $BaTiO_3$ pellets are compared to those obtained by conventional sintering of $BaTiO_3$ ceramics as well as to SPS $BaTiO_3$ ceramics produced from powders prepared from hydrothermal synthesis.

2. Experimental procedure

$BaTiO_3$ powders were prepared by a sol-crystal method [21]. Guaranteed-reagent-grade barium metal (99.9% pure) was reacted with isopropyl alcohol (reagent grade) in a mixed solution of isopropyl alcohol and benzene (reagent grade) in which titanium tetraisopropoxide ($Ti[OCH(CH_3)_2]_4$; reagent grade) was dissolved. All solvents were dried with CaH_2 and distilled *in vacuo* prior to use. The reaction was conducted at 40°C under an argon atmosphere with stirring until the barium metal was completely dissolved. The reaction vessel was stoppered and left at 5°C, which led to crystal growth in the solution. The crystals were separated from the solution and dried in an argon atmosphere, which led to decomposition into a white powder (hereafter called as-prepared powder). The as-prepared powder was subsequently sintered in the form of discs by SPS using an SPS-2040 (Izumi Technology) [19, 20] or by conventional heating in a muffle furnace.

For SPS sintering, $BaTiO_3$ powder (ca. 2 g) was placed into a graphite die (15 mm in diameter) and an electric current of ca. 1000 A was applied under a pressure of 39 MPa. During this procedure, the temperature increased to 900 or 1000°C at a rate of ca. 200°C/min (controlled by the applied current). After it was kept at the desired temperature for ca. 3 min, the applied electric current was switched off, the pressure released and the sample cooled to room temperature. Within 1 min of the cooling cycle, the temperature dropped to ca. 600°C. The as-sintered pellets (15 mm in diameter and 2 mm thick) were annealed in air at 900°C for 2 h (SPS-pellets). For the conventional heating process, as-prepared $BaTiO_3$ powder was pressed into pellets under a pressure of 190 MPa and subsequently sintered in air for 2 h at 1000, 1200, 1300 or 1400°C (CS-pellets).

Phase purity and composition of the pellets were checked by X-ray diffractometry (Rigaku RINT-1500 using Cu K_α radiation), infrared spectroscopy (Horiba FT-200) and field emission scanning electron microscopy (FE-SEM; Hitachi S-5000) with energy dispersion X-ray (EDX) microanalysis (Horiba EMAX-5770W). The Ba and Ti contents of the pellets were determined by inductively coupled plasma (ICP) emission spectroscopy. Thermogravimetry (Rigaku TAS200) was employed to monitor any weight changes on re-oxidation of the pellets prepared from the SPS method. Pellet densities were determined using Archimedes method after the pellets were soaked in the boiling water for 1 h to eliminate the influence of surface micropores. To determine the average grain size (diameter), at least 200 grains were chosen and the grain size distributions were measured using a computerized image analyzer (EXCEL, Nippon Avionics).

The electrical permittivity measurements were carried out using Solartron 1260 instrumentation, covering the frequency range 10^{-2} to 10^6 Hz. Prior to electrical measurements, pellets were coated with Au paste electrodes (Engelhard A-3360) which were fired at 700°C. All samples were measured over the temperature range 25–300°C, with equilibration periods of 15 min at each temperature. All electrical measurements were corrected for pellet geometry.

3. Results and discussion

X-ray diffraction patterns of as-sintered SPS pellets showed the presence of graphite contamination from the carbon die, but not in the post-annealed pellets. The EDX results further confirm the removal of carbon contamination by annealing; no carbon $K\alpha$ peak was detected after annealing in air. Thermogravimetry showed a weight loss of ca. 0.3 wt% on heating to 900°C in air and no weight loss from 900 to 1200°C, probably due to the elimination of graphite in the form of gaseous CO and/or CO_2. IR spectra showed the peaks originated from H_2O, $BaCO_3$ and organic compounds (e.g., stretching and deformation modes for CH-groups) in the as-prepared powder, as reported previously [24], but these impurities were not detected in the SPS and CS pellets.

SPS pellet densities after annealing are plotted as a function of sintering temperature in Fig. 1a.

Relatively dense pellets ($>95\%$ of the theoretical X-ray density) were obtained by the SPS process. On the contrary, CS pellets sintered at 1000–1300°C showed lower density (72–94% of the theoretical X-ray density) than those of the SPS pellets, and high density (97%) can only be achieved at much higher sintering temperatures, for example, 1400°C. As compared with our previous SPS $BaTiO_3$ pellets (sintered at $>1000°C$) starting from submicrometer-sized powders (0.1–0.6 μm) prepared by hydrothermal and hydrolysis methods [19, 20], high density ($>95\%$) SPS pellets were obtained at relatively lower temperature (900–1000°C), owing mainly to the fine $BaTiO_3$ powder (several

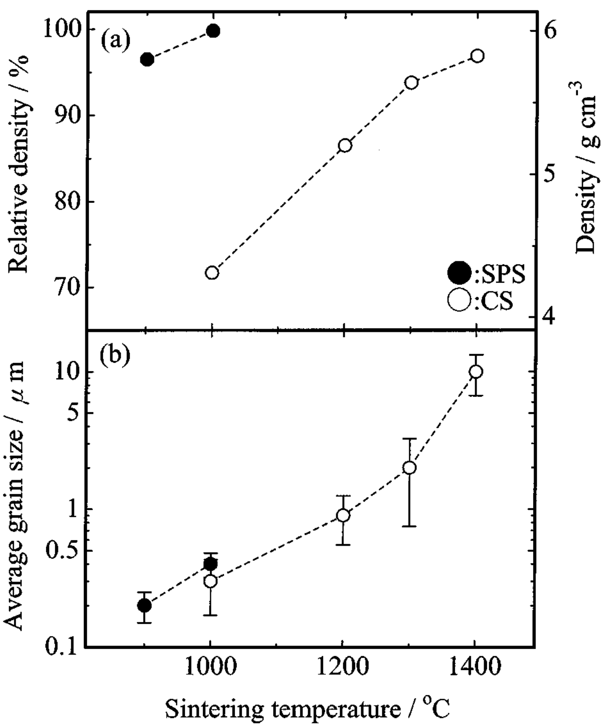

Figure 1 (a) Relative density and (b) average grain size for SPS and CS pellets as a function of sintering temperature.

nanometers) [21, 24] obtained from the sol-crystal method. Ba and Ti contents estimated from ICP emission spectroscopy were 57.9(±1.7) and 19.5(±0.6) for SPS pellets sintered at 900°C and 57.2(±1.7) and 19.2(±0.6) for those sintered at 1000°C. These values are in good agreement with the theoretical values of 58.9 and 20.5 for Ba and Ti, respectively.

Typical SEM micrographs of fracture surfaces of annealed SPS pellets are shown in Fig. 2a.

The SPS pellets consist of submicron (0.1–1 μm) grains, and the grain size depends on the sintering temperature; average grain size increases with sintering temperature, as shown in Fig. 1b. SPS was also performed at 1000°C for 30 min, and exaggerated grain growth with average grain sizes in excess of 10 μm were observed. These results show the necessity of short sintering period to obtain $BaTiO_3$ ceramics with submicron grains via SPS. For comparison, SEM micrographs of typical CS pellets are shown in Fig. 2b. In contrast to the SPS pellets, the average grain size of these pellets increased to more than 1 μm due to much longer sintering period (2 h).

Typical fixed-frequency, 1 kHz, permittivity data for SPS and CS pellets over the temperature range 25–300°C are shown in Fig. 3.

Both show a clear permittivity maximum at the Curie temperature, ca. 130°C. SPS pellets sintered at 1000°C show higher permittivity values, particularly below the Curie temperature, where their room temperature permittivity is ca. 10000, compared to ca. 4500 for CS pellets. The higher permittivity values for SPS (1000°C) pellets may be associated with their higher density and the restricted grain growth. However, dissipation factors (tan δ) at 1 kHz for SPS (1000°C) pellets were relatively high (16–21% at 25–300°C), suggesting the presence of oxygen deficiency (reduction) in SPS samples, as discussed later. Low permittivity values for CS pellets sintered above 1300°C (typically 1000–2000 at room temperature, not shown) may be associated with the decrease in surface area of the 90° ferroelectric domain walls in large $BaTiO_3$ grains [4, 8, 9].

Fig. 4 shows the frequency dependence of the room temparature permittivities for SPS and CS pellets.

Data for CS (1200°C) pellets show the presence of a plateau above ca. 10^2 Hz, whereas data for SPS (1000°C) pellets show a moderate slope in permittivity in the low frequency region, no well defined high frequency plateau (10^3–10^5 Hz) and a plausible beginning for a high frequency ($>10^6$ Hz) plateau. Hirose and West [25] have shown the high frequency permittivity plateau (>ca. 10^3 Hz) is dominated mainly by the permittivity of the grains and less from the permittivities associated with grain boundaries and air gaps. Permittivity data at 1 kHz for SPS (1000°C) pellets lie in the intermediate (dispersion) region and are therefore an overestimation of the grain permittivity [20, 25], and explains the apparently high permittivity of (unpolished) SPS (1000°C) pellets, Fig. 3. Closer inspection of AC impedance data was undertaken in an attempt to examine the origin of the unusual frequency dependence of permittivity for SPS (1000°C) pellets.

Representative combined Z'' (imaginary part of complex impedance Z^*) and M'' (imaginary part of complex modulus M^*) [26] spectroscopic plots for SPS (1000°C) pellets at 300°C are shown in Fig. 5a.

The Z'' plot shows a single Debye-like peak with a frequency maximum ($f_{\max}$) value at 0.6 Hz. In contrast, the M'' plot shows two peaks with $f_{\max}$ values of 1.3 and 730 Hz, respectively. Since Z'' spectra are dominated by components with large resistance and M'' spectra by those with small capacitance [26], Fig. 5a suggests that SPS (1000°C) pellets consist of high and low resistive components with similar capacitance values. Indeed, resistances are calculated as 120 and 0.2 MΩ and capacitances as 1.6 and 1.4 nF for low and high frequency components at 300°C, respectively, using the relationships $Z''_{\max} = R/2$, $M''_{\max} = C_0/2C$, and $\omega RC = 1$ at peak maximum, where C_0 is the vacuum capacitance of the cell and ω is angular frequency [26]. Since no impurity phases were observed in XRD and IR and no elements other than Ba, Ti and O were detected by EDX for SPS (1000°C) pellets, the high frequency component (low resistance) must be associated with oxygen deficient (slightly reduced) $BaTiO_3$ whereas the low frequency component (high resistance) must be associated with $BaTiO_3$ which has very little (if any) oxygen deficiency.

Two plausible models can be proposed for the coexistence of $BaTiO_3$ and reduced $BaTiO_3$ ($BaTiO_{3-\delta}$, where δ is oxygen deficiency); (i) each grain in the SPS pellets consists of outer $BaTiO_3$ regions and inner reduced $BaTiO_{3-\delta}$ cores or (ii) pellets surfaces consist of $BaTiO_3$ whereas the interior of the pellets consist of $BaTiO_{3-\delta}$ (see Fig. 6).

In an attempt to distinguish between these two models, SPS (1000°C) pellets were polished (ca. 0.2 mm depth) and the electrical properties remeasured. Fig. 5b shows a typical combined Z'', M'' spectroscopic plot

(a) SPS 1000°C 3min

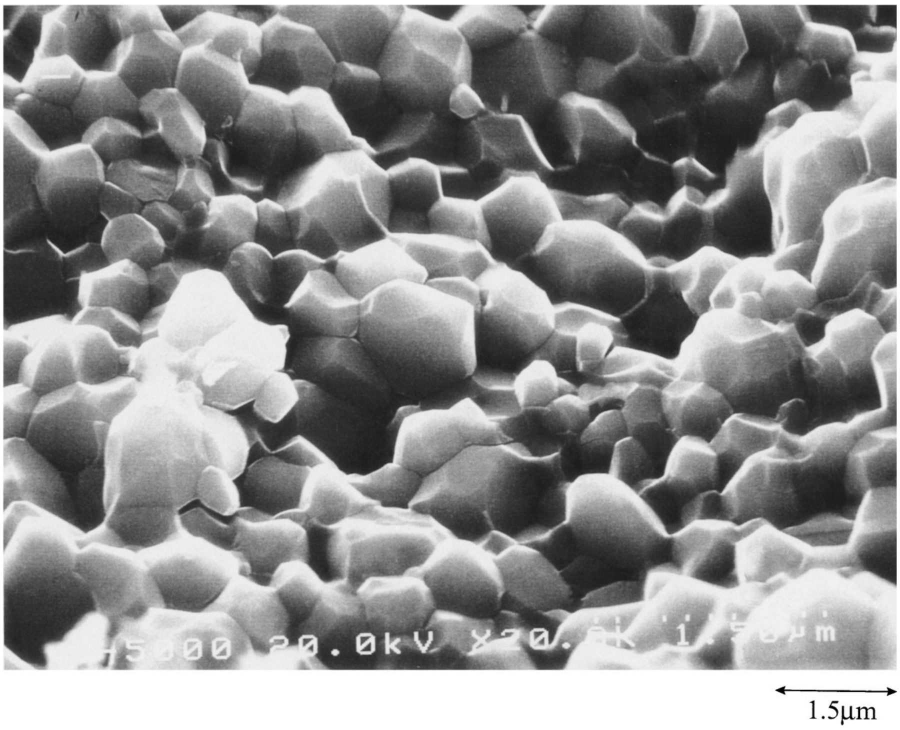

(b) CS 1200°C 2h

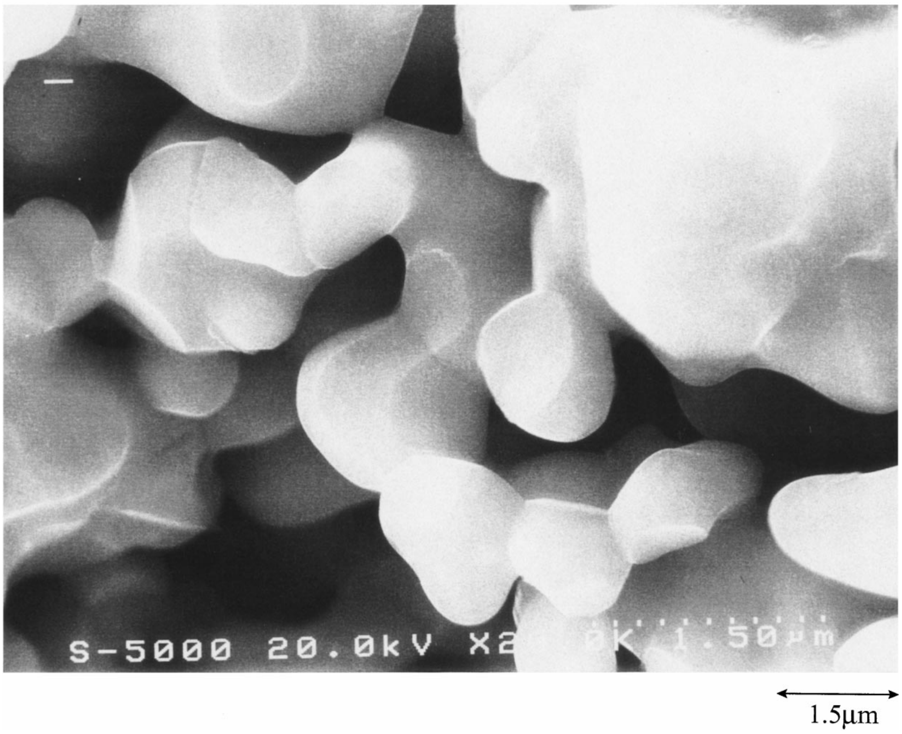

Figure 2 SEM micrographs of fracture surfaces for (a) SPS and (b) CS pellets with different sintering conditions. Magnification is the same for both micrographs.

at 300°C for a polished SPS (1000°C) pellet. The Z'' plot shows the peak to have shifted to higher frequency ($f_{\max} = 560$ Hz) and a drastic decrease in the peak height ($Z''_{\max} = 160$ kΩ) has occurred, leading to a decrease in total resistance of the pellet. The corresponding M'' plot shows a rather diffuse, broad peak with $f_{\max} = 16$ kHz with $M''_{\max}$ similar in value to that of non-polished pellets, Fig. 5a. The spectra clearly demonstrate that polishing SPS (1000°C) pellets reduces the contribution from more resistive components to the total electrical properties. This experimental result disagrees with the model (i), in which Z'' and M'' plots should not change largely after polishing the pellets. Therefore, SPS (1000°C) pellets can be considered to be composed of a surface layer of re-oxidized $BaTiO_3$ which covers the inner pellet core consisting of reduced $BaTiO_{3-\delta}$. Permittivity values for the polished SPS (1000°C) pellets are also shown in Figs 3 and 4. The frequency dependence of the permittivity shows a plateau in high frequency region ($\geqq 10^3$ Hz, including

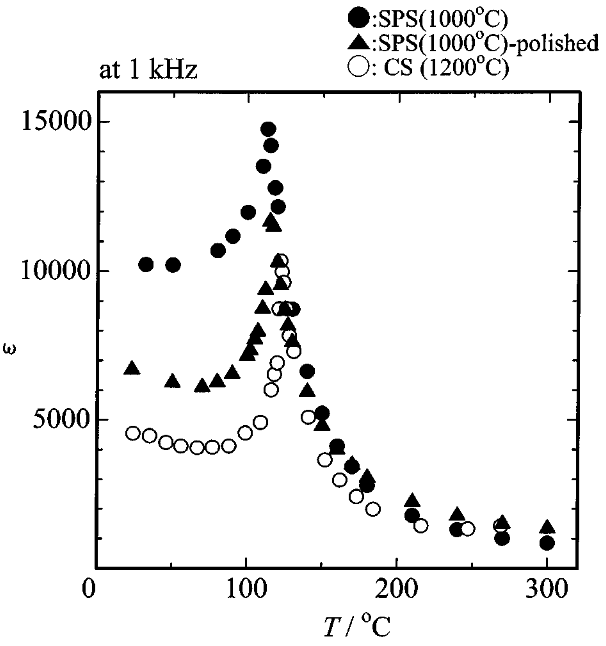

Figure 3 Temperature dependence of dielectric constants at 1 kHz for SPS and CS pellets with different sintering conditions.

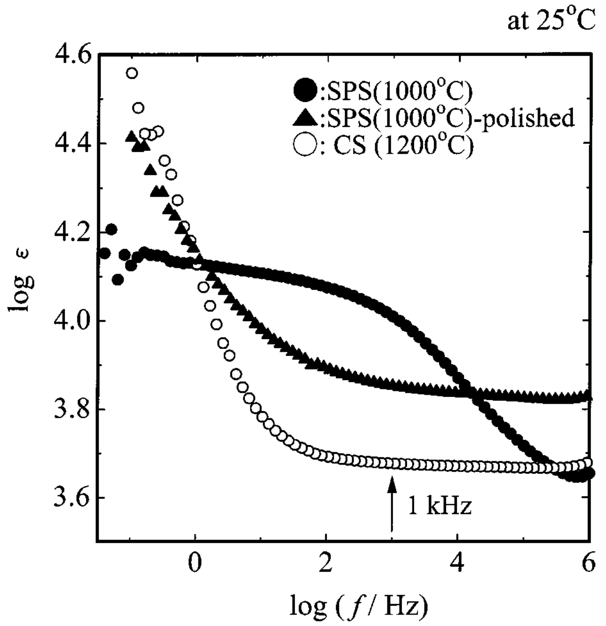

Figure 4 Frequency dependence of permittivities at 25°C for SPS and CS pellets with different sintering conditions.

1 kHz), suggesting almost no overestimation of grain permittivity at 1 kHz [20, 25]. Indeed, room temperature permittivity at 1 kHz of the SPS pellets decreases after polishing, Fig. 3, but the value is still higher than that of CS pellets, which may be due to the higher density of the SPS pellets.

$BaTiO_{3-\delta}$ might be formed during the SPS process by elimination of organic compounds (which are present in the starting powder) in the form of gaseous CO and/or CO_2. The dense pellets are therefore not completely re-oxidized by annealing at 900°C for 2 h after the SPS process. Since AC impedance data for SPS (1000°C) pellets annealed at 900°C for 24 h showed similar spectroscopic plots to Fig. 5a, preparing fully re-oxidized pellets appears to be difficult, probably because of slow oxygen migration inside the dense pellets. In other word, the present non-polished SPS pellets would be stable on exposure to air for a long period. Thickness of the surface $BaTiO_3$ layer of the SPS pellets seems to be less than ca. 0.2 mm, since AC impedance data

(a) SPS (1000°C 3min)

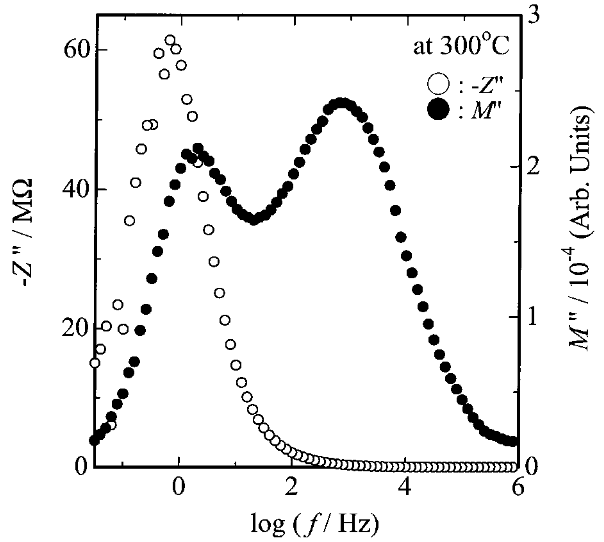

(b) SPS (1000°C 3min) - polished

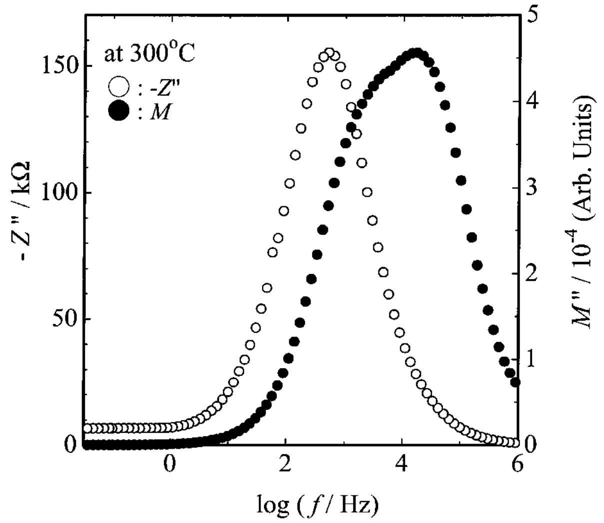

Figure 5 Combined $-Z''$ and M'' spectroscopic plots at 300°C for (a) SPS pellet sintered at 1000°C for 3 min and (b) its polished pellet.

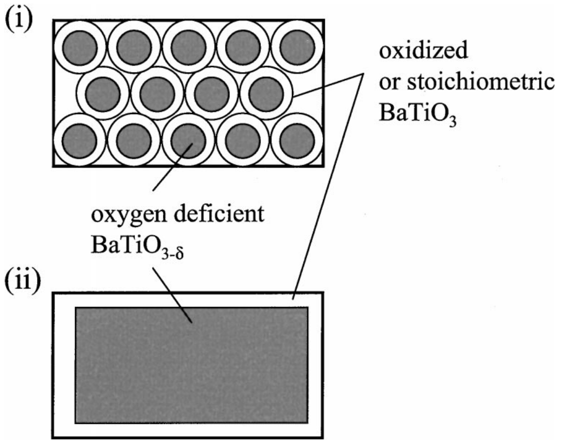

Figure 6 Schematic representation of two plausible models for SPS $BaTiO_3$ pellets prepared from powders that contain residual organic matter. White area represents oxidized or stoichiometric $BaTiO_3$, and hatched area represents oxygen deficient $BaTiO_{3-\delta}$. See text.

for further polished (>ca. 0.3 mm depth) SPS (1000°C) pellets showed almost no changes from those of Fig. 5b. Our previous SPS $BaTiO_3$ pellets starting from powders without organic compounds did not show such an unusual frequency dependent permittivity behavior, Fig. 4, for non-polished pellets [19, 20]. Reduced $BaTiO_{3-\delta}$ pellets are a characteristic of SPS processing when starting from powders that contain residual organic compounds. This layered pellet structure (fully oxidized and reduced $BaTiO_3$) is similar to that of barrier layer capacitors, where semiconducting (reduced) barium and/or strontium titanate grains are surrounded by thin oxidized surface layers, either as a skin on the pellet or in the form of grain boundary/outer grain regions [1]. Thus combining SPS with $BaTiO_3$ powders containing residual organic matter may be a novel method for manufacturing $BaTiO_3$-based barrier layer capacitors.

4. Conclusions

We have applied Spark-Plasma-Sintering method to fine $BaTiO_3$ powder (several nanometers) prepared by a sol-crystal method to obtain dense pellets (>95% of the theoretical X-ray density) with an average grain size of less than ca. 1 μm at relatively lower sintering temperature (900–1000°C). The apparent room temperature permittivity at 1 kHz attains to ca. 10000 for SPS (1000°C) samples. This apparently high permittivity value is attributed to electrical inhomogeneity within pellets; a thin fully oxidized $BaTiO_3$ surface layer covers the inner pellet core which consists of oxygen deficient $BaTiO_{3-\delta}$. This method of combining SPS processing with fine $BaTiO_3$ powders that contain residual organic matter may be an alternative method to produce barrier layer capacitor ceramics based on $BaTiO_3$.

Acknowledgments

We wish to express our gratitude to Mr. Masakazu Kawahara and Dr. Masao Tokita of Izumi Technology for their help with spark plasma sintering.

References

1. J. NOWOTNY and M. REKAS, *Key Engineering Materials* **66/67** (1992) 45.
2. I. J. CLARK, T. TAKEUCHI, N. OHTORI and D. C. SINCLAIR, *J. Mater. Chem.* **9** (1999) 83.
3. K. KINOSHITA and A. YAMAJI, *J. Appl. Phys.* **47** (1976) 371.
4. D. HENNINGS, *Int. J. High Technology Ceramics* **3** (1987) 91.
5. A. S. SHAIKH, R. W. VEST and G. M. VEST, *IEEE Trans. Ultraso. Ferroelec. Frequency Control* **36** (1989) 407.
6. G. CABOCHE and J. C. NIEPCE, in “Ceramic Transactions,” vol. 32, “Dielectric Ceramics: Processing, Properties, and Applications,” edited by K. M. Nair, J. P. Guha and A. Okamoto (American Ceramic Society, Westerville, OH, 1993) p. 339.
7. T. OTA, J. TAKAHASHI and I. YAMAI, *Key Engineering Materials* **66/67** (1992) 185.
8. J. C. NIEPCE, in “Surface and Interface of Ceramic Materials,” edited by L. C. Dufour, C. Monty and G. Petot-Ervas (Kluwer, Dordrecht, Germany, 1989) p. 521.
9. G. ARLT, D. HENNINGS and G. DE WITH, *J. Appl. Phys.* **58** (1985) 1619.
10. K. UCHINO, E. SADANAGA and T. HIROSE, *J. Amer. Ceram. Soc.* **72** (1989) 1555.
11. M. H. FREY and D. A. PAYNE, *Phys. Rev. B* **54** (1996) 3158.
12. M. H. FREY, Z. XU, P. HAN and D. A. PAYNE, *Ferroelectrics* **206/207** (1998) 337.
13. K. OONISHI, T. MOROHASHI and K. UCHINO, *J. Ceram. Soc. Japan* **97** (1989) 473.
14. W. R. BUESSEM, L. E. CROSS and A. K. GOSWAMI, *J. Amer. Ceram. Soc.* **49** (1966) 36.
15. G. A. SAMARA, *Phys. Rev.* **151** (1966) 378.
16. M. TOKITA, *J. Soc. Powder Tech. Jpn.* **30** (1993) 790.
17. I. KONDOH, T. TANAKA and N. TAMARI, *J. Ceram. Soc. Japan* **102** (1994) 505.
18. N. TAMARI, T. TANAKA, K. TANAKA, I. KONDOH, M. KAWAHARA and M. TOKITA, *J. Ceram. Soc. Japan* **103** (1995) 740.
19. T. TAKEUCHI, M. TABUCHI, H. KAGEYAMA and Y. SUYAMA, *J. Amer. Ceram. Soc.* **82** (1999) 939.
20. T. TAKEUCHI, E. BÉTOURNÉ, M. TABUCHI, H. KAGEYAMA, Y. KOBAYASHI, A. COATS, F. MORRISON, D. C. SINCLAIR and A. R. WEST, *J. Mater. Sci.* **34** (1999) 917.
21. Y. SUYAMA and M. NAGASAWA, *J. Amer. Ceram. Soc.* **77** 603 (1994).
22. Y. SUYAMA, T. NORITAKE and M. NAGASAWA, *Jpn. J. Appl. Phys.* **36** (1997) 5939.
23. K. W. KIRBY, *Mater. Res. Bull.* **23** (1988) 881.
24. T. TAKEUCHI, M. TABUCHI, K. ADO, K. HONJO, O. NAKAMURA, H. KAGEYAMA, Y. SUYAMA, N. OHTORI and M. NAGASAWA, *J. Mater. Sci.* **32** (1997) 4053.
25. N. HIROSE and A. R. WEST, *J. Amer. Ceram. Soc.* **79** (1996) 1633.
26. D. C. SINCLAIR and A. R. WEST, *J. Appl. Phys.* **66** (1989) 3850.

Received 21 December 1999
and accepted 4 October 2000